METASTABLE LIMIT DYNAMICS AND OPTIMAL COOLING CURVE OF BATCH SEEDED CRYSTALLIZATION

Seunghee Won,* Kwang S. Lee,*,[1] Chung S. Choi*
Ju-Seok Lee Daeryook Yang****

* *Dept. of Chem. and Biomol. Eng., Sogang University*
1 Shinsoodong, Mapogu, Seoul 121-742, Korea
** *Dept. of Chem. and Bio. Eng., Korea University,*
Anamdong, Seongbukgu, Seoul, Korea

Abstract: For seeded cooling crystallization, itn is required that the solution is maintained at a supersaturation state within the metastable limit for suppression of homogeneous nucleation. However, the metastable limit is not fixed but time-varying depending upon the solution history. In this study, dynamics of the metastable limit has been exploited. Using the experimental results obtained under various cooling rates, the metastable limit was expressed to have a nonlinear first-order dynamics to a change in the cooling rate. By incorporating this model, an optimal cooling curve was determined for $(NH_4)_2SO_4$ crystallization from the $(NH_4)_2SO_4$-NH_4NO_3-H_2O ternary system and experimental verification has been performed.

Keywords: Batch Crystallization, Cooling Crystallization, Metastable Limit, Batch Model Predictive Control

1. INTRODUCTION

Crystallization is an indispensable separation and purification process in chemical and related industries. As the biochemical and pharmaceutical industries grow fast recently, importance of the crystallization process has been recognized more. Nevertheless, many aspects of crystallization are not understood well and the industrial crystallization is still regarded as an art.

In industrial crystallization, size uniformity of the final product is very often the most important quality requirement. For this, seeded cooling crystallization is widely practiced while carefully controlling the solution state to remain within the metastable limit. However, the metastable limit is not given as a fixed property of a solution but varies with time. Sometimes it is sensitively affected by various disturbances such as agitation and impurities. If the metastable limit can be accurately identified, one can push the solution to the limit so that the rate of crystal growth, *i.e.* the productivity, is maximized while suppressing the homogeneous nucleation. There have been researches to describe the time-varying behavior of the metastable limit. It is Nývlt and his research group who had pioneered the issue for a long period(Nývlt *et al.*, 1970)(Nývlt, 1983). They suggested different nonlinear models that relate the cooling rate to the metastable limit. On the basis of Nývlt's study, Choi and Kim(1991) suggested an improved correlation. From the system theoretic point of view, the above researches can be interpreted as an attempt to represent the dynamics of the metastable limit as a nonlinear

[1] All correspondence should be addressed to: phone +82-2-705-8477, fax +82-2-3272-0319, e-mail kslee@sogang.ac.kr

integral process to the solution temperature. As will be explained later, however, the existing models can be refined further if a system theoretic representation can be incorporated.

In this research, a new dynamic model that describes the time-varying behavior of the metastable limit is proposed for seeded cooling crystallization. For this, experimental results in a literature obtained for $(NH_4)_2SO_4$ crystallization from the $(NH_4)_2SO_4$-NH_4NO_3-H_2O ternary system have been reinterpreted and a nonlinear first-order dynamic model has been derived as a relationship between the cooling rate and the metastable limit. On the basis of this result, an optimum cooling curve that provides the maximum productivity without homogeneous nucleation is determined. Experiments have been performed in a batch crystallizer to verify the theoretic prediction.

2. BEHAVIOR OF METASTABLE LIMIT AND DYNAMIC MODELING

2.1 Basic Notions

The basic notions related to the cooling crystallization can be described in the solubility-supersolubility diagram as in Fig. 1. The solubility curve of a solution is well defined thermodynamically and can be determined through experiments. The solute is precipitated when the solution moves out of the stable zone. When the solution is in the metastable zone, only the seeded heterogeneous nucleation takes place whereas the homogeneous nucleation can occur in the labile zone. Therefore,

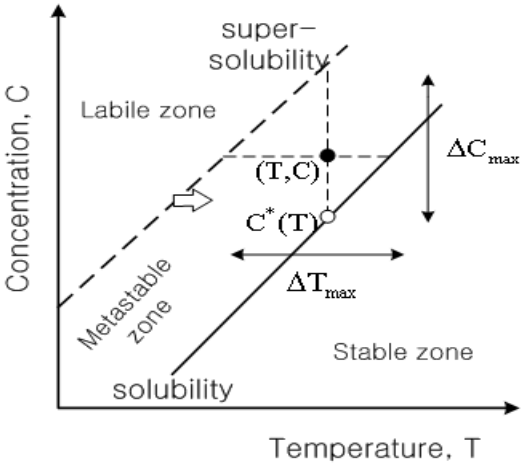

Fig. 1. Solubility-supersolubility diagram.

if the initial seed size is uniform; the solution is retained in the metastable zone during the crystal growth; and the undesired secondary nucleation can be suppressed by appropriate design of the crystallizer, then we can obtain uniform-size crystal product. Due to the above reason, the metastable zone is where the industrial crystallization is carried out. The boundary dividing the labile and metastable zones is called the metastable limit or supersolubility curve.

For a certain solution state (T, C) in the metastable zone, $C - C^*(T)$ where $C^*(T)$ is the concentration on the solubility curve represents the driving force for the crystal growth. In the figure, $\Delta C_{max}(T)$ is called the maximum allowable supersaturation (MASS) at T. Likewise, $\Delta T_{max}(C)$ is called the maximum allowable undercooling (MAUC) at C. Either MASS or MAUC is used to define the metastable zone width.

2.2 Dynamic Behavior and Mathematical Modeling

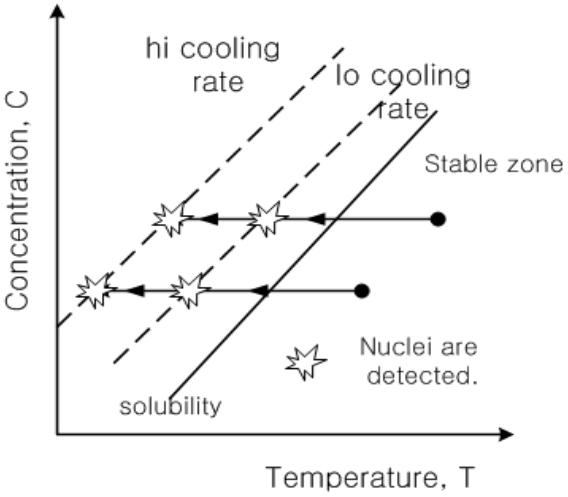

Fig. 2. Solubility-supersolubility diagram.

Unlike the solubility curve, the supersolubility (SS) curve (or metastable limit) is not fixed but time-varying depending on the solution history. Obviously, the SS curve coincides with the solubility curve at an equilibrium. This implies that the curve gradually moves toward the solubility curve as time elapses if the solution is kept undisturbed. To illustrate this, suppose that a solution is at (T, C) in Fig. 1 and the SS curve is given as in the figure at the initial time. Since the solution is in the metastable zone, no homogeneous nucleation takes place. As time goes, however, the metastable limit shifts to the right and eventually the nuclei come out at the moment when it touches the point (T, C). The time-varying behavior can also be investigated under constant cooling experiments. As shown in Fig. 2, if the solution in the stable zone is cooled at a constant rate, nuclei appear at a certain point beyond the solubility curve. When the cooling rate is high, nuclei appear at a lower temperature than the case for a low cooling rate.

This implies that the metastable limit is pushed back farther at a higher cooling rate.

Nývlt (1983) has proposed the following relationship between the cooling rate and the MAUC:

$$\Delta T_{max} = ku^p \tag{1}$$

where $u \triangleq -dT/dt$ is the cooling rate. In terms of ΔC_{max}, Choi and Kim (1991) have proposed the relationship

$$\Delta C_{max} = k_0 u^{k_1} + k_2(T_0 - T) \tag{2}$$

where T_0 is the initial temperature of the solution.

From the system theoretic point of view, eqs. (1) and (2) can be interpreted as nonlinear integral dynamic models to a change in the solution temperature. However, the representations can be more complete if we consider two thought experiments as depicted in Fig. 3. First, consider the case (a) where the solution temperature drops stepwise. If eq. (1) holds, ΔT_{max} will change as an impulse function, which is improbable. A more reasonable response of ΔT_{max} would be a sudden increase followed by a slow decay as shown in the figure. As a next case, consider that the solution temperature decreases at a constant rate from an initial rested state. According to eq. (1), ΔT_{max} increases stepwise at the initial time. Such a sudden increase is unreasonable in a physical system and a better description would be a smooth increase as in Fig. 3(b).

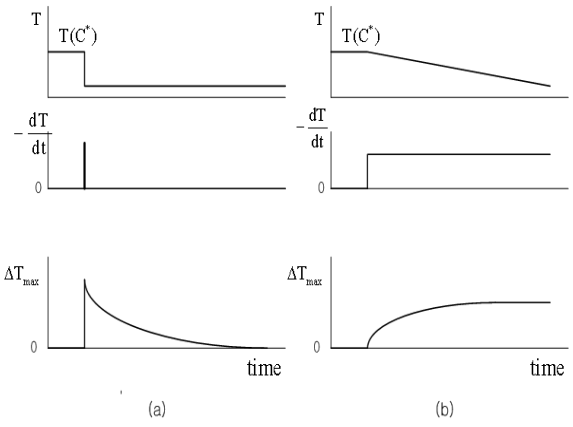

Fig. 3. Imagined responses of the metastable limit to changes in the solution temperature.

The responses in Fig. 3 are in fact those of the first-order lag dynamics. Incorporating the nonlinear steady state relationship as in eq. (1), we propose the following dynamic model for ΔT_{max}:

$$\begin{aligned} \tau \frac{dx}{dt} + x &= u \\ \Delta T_{max} &= kx^p \end{aligned} \tag{3}$$

Integrating the above yields

$$\Delta T_{max}(t) = k\left(u(1 - e^{-t/\tau})\right)^p \tag{4}$$

The parameters can be determined from the experimental data to best fit the above model.

3. COOLING CURVE OPTIMIZATION

3.1 Governing Equations for Batch Crystallizer

The mass balance equation for the concentration of the dissolved solute, C, under negligible homogeneous nucleation can be written as (Choi and Kim, 1991)

$$\frac{dC}{dt} = -\theta \frac{W_{s_0}}{L_{s_0}^3} \exp\left(-\frac{E}{RT}\right) L^{2+d}(C - C^*)^g \tag{5}$$

where

$$L = \left(L_{S_0}^3 - \frac{L_{S_0}^3}{W_{S_0}}(C_0 - C)\right)^{1/3} \tag{6}$$

In the above, L and W represent the characteristic size and weight of the crystal, respectively; the subscript S_0 means the initial seed. Under the assumption that there is no homogeneous primary and secondary crystallization, decrease in C can be converted to the size increase of the crystal through eq. (6).

Now, eq. (5) and the cooling rate equation

$$\frac{dT}{dt} = -u \tag{7}$$

constitute the overall unsteady dynamic equations (between u and L) for the crystallizer.

3.2 Working Supersaturation Level

Eq. (3) defines the allowable zone for the solution temperature without incurring homogeneous nucleation. In real crystallizers, spatial distribution of solution temperature is unavoidable. Especially, the solution temperature near the coolant inlet is lower than the bulk temperature, which means that nucleation may burst at such cold spots even though the bulk temperature remains within the allowable limit. In addition, the model parameters in eq. (3) may contain unnegligible errors since it is hard to obtain reliable experimental data in crystallization. Due to the above reasons, it is risky to push the solution temperature to the theoretical metal stable limit predicted by eq. (3). Instead, it is necessary to give some safety margin. For this, we introduce the concept of working supersaturation level $0 \leq \eta \leq 1$ as follows:

$$\eta \triangleq \frac{T^*(C) - T}{\Delta T_{max}} \tag{8}$$

3.3 Objective Functions

We consider the following cooling curve optimization which maximizes the resulting crystal size over a specified period of batch operation:

$$\max_{u(\cdot)} L(t_f, u(\cdot)) \quad \Leftrightarrow \quad \min_{u(\cdot)} C(t_f, u(\cdot)) \tag{9}$$
$$\text{subject to } 0 < \eta \leq \eta_{max} \text{ and eqns. (5)-(8)}$$

A penalty function method was used to solve the above problem.

4. NUMERICAL STUDY

We consider the crystallization of $(NH_4)_2SO_4$ in $(NH_4)_2SO_4$-NH_4NO_3-H_2O ternary system with 28wt% of NH_4NO_3, which has been studied by Choi and Kim(1990, 1991). The parameters for eq. (3) were determined using the published data in Choi and Kim (1991) obtained from constant cooling rate experiments. Since there is a strong dependency of the parameters on the solution concentration, the parameter estimates were represented as linear functions of concentration such as $\tau = \tau_1 + \tau_2 C$ and so forth. Other parameters for eqns. (5) and (6) and the solubility curve were imported from Choi and Kim (1991).

Figures 4-6 show the numerical results when the seed crystal of $W_{S_0} = 8.1$ g/kg-solution and $L_{S_0} = 0.45$ mm is used and $\eta_{max} = 0.5$ is assumed. During the optimization, an additional condition that the maximum cooling is limited by 90°C/hr was superimposed. The batch operation time was chosen to be 60 min.

As shown in Fig. 4, the estimated optimum cooling curve has a fast temperature decrease at the initial time. It is contrary to the usual industrial practice where the solution is cautiously and slowly cooled at beginning of the operation. As can be seen from from Fig. 2, however, a faster cooling rate can push back the metastable limit farther. Considering this, fast cooling at the initial time widens the metastable zone and enables the ensuing operation to be carried out with large concentration driving force $C(T) - C(T^*)$. Figure 5 shows the associated metastable limit estimate from the optimum cooling curve. It can seen that the metastability limit is pushed back at first by the initial temperature drop and then pulled back as time elapses. After the initial transient, the solution temperature decreases at an appropriate rate maintaining the specified working supersaturation level. Figure 6 shows the profile of the supersaturation level η. During an initial period, the cooling rate is on the constraint limit and η has a value around 0.3. After the period, η increases and stays close to 0.5. Obviously, $C(T) - C(T^*)$ is maximum when $\eta(T) = \eta_{max}(T)$.

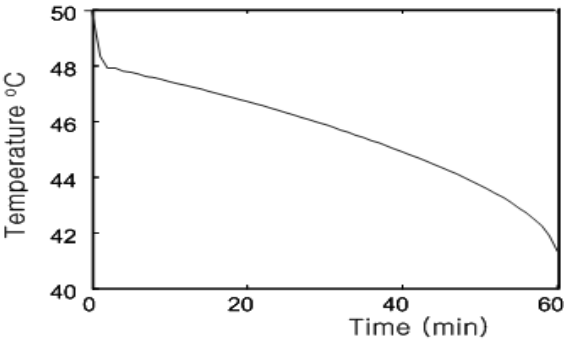

Fig. 4. Optimum cooling curve for $W_{S_0} = 8.1$g/kg and $\eta_{max} = 0.5$.

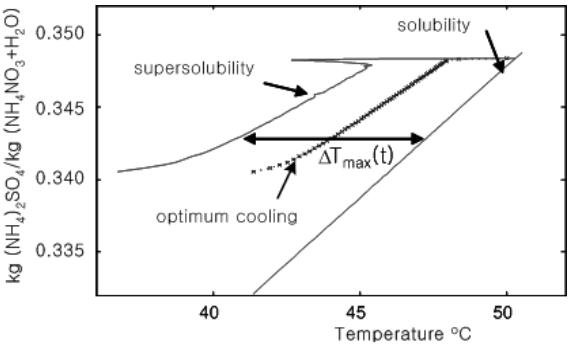

Fig. 5. Resulting supersolubility curve.

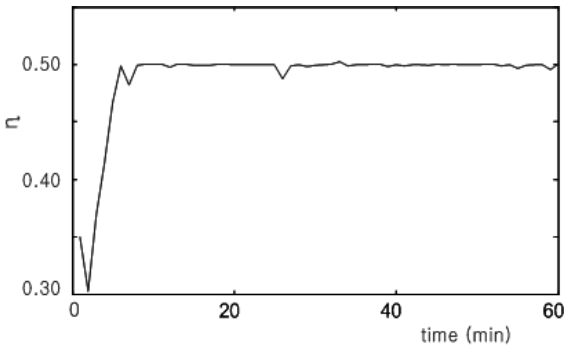

Fig. 6. Supersaturation level profile.

In Figs. 7 and 8, effects of the amount of the seed crystal and η_{max} are shown, respectively. As the amount of seed crystal increases, desupersaturation is enhanced and a higher cooling rate is required. On the other hand, as η_{max} is lowered, a smaller concentration driving force is allowed resulting in a slower cooling rate.

In Fig. 9, three cooling curves, optimum, linear, and natural, are compared for $W_{S_0} = 8.1$g/kg and $\eta_{max} = 0.5$. In Fig. 10, the associated metastable

limit is shown for the linear cooling case for $\eta_{max} = 0.5$. It is observed that the condition $\eta \leq \eta_{max}$ is violated, which tells that homogeneous nucleation may be brought about during the operation. Though not shown here, the natural cooling also violates the working supersaturation condition.

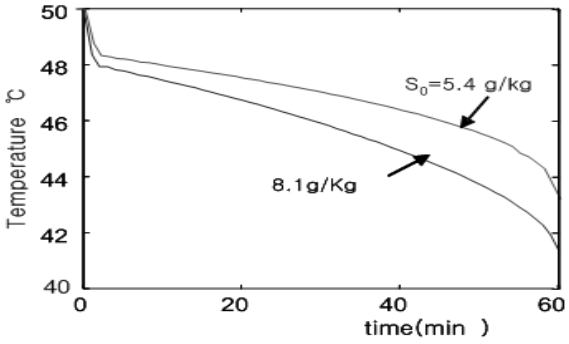

Fig. 7. Effects of initial seed amount on the optimum cooling curve.

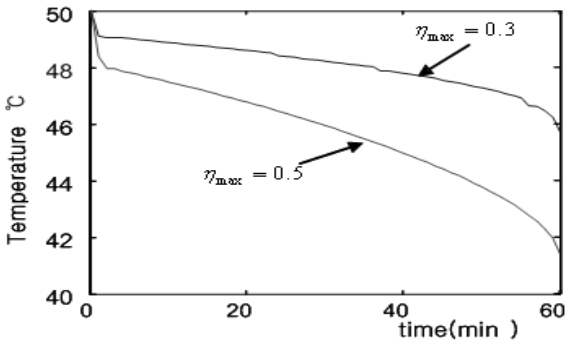

Fig. 8. Effects of η_{max} on the opt. cooling curve.

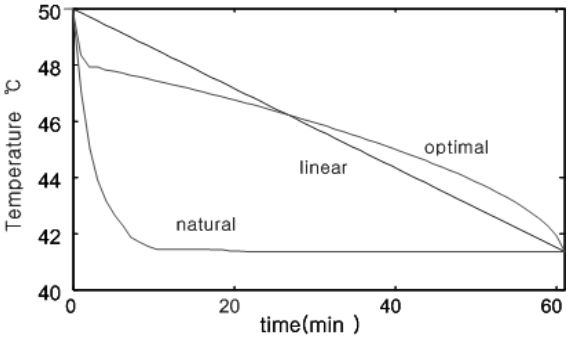

Fig. 9. Optimum, linear, and natural cooling curves for $W_{S_0} = 8.1$g/kg and $\eta_{max} = 0.5$.

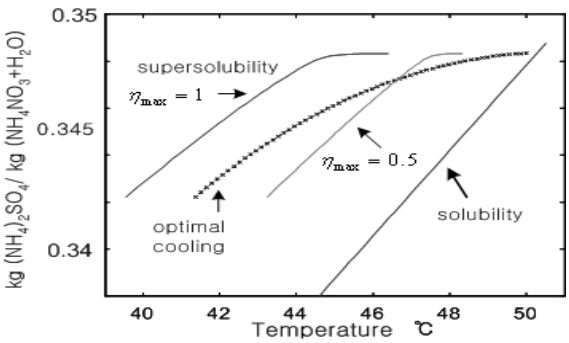

Fig. 10. Supersolubility curve for linear cooling.

5. EXPERIMENTAL STUDY

5.1 Experimental Setup

To verify the proposed optimum cooling curve, experiments have been conducted in a 2.5 liter batch crystallizer. In order to prevent breakage and secondary nucleation, the crystallizer has a hollow draft tube where the agitation impeller rotates at the center of the draft tube and crystals are confined and grown in the annulus section between the draft tube and the vessel wall. Figure 11 shows the schematic diagram of the experimental setting. Temperature was measured with thermocouples calibrated with a high precision thermometer.

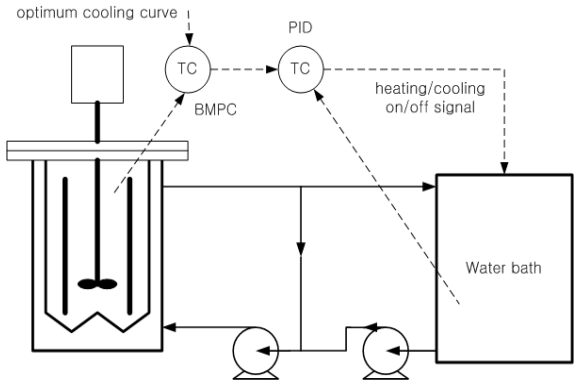

Fig. 11. Experimental set-up.

5.2 Experimental Condition

In the experiments, 2 kg of $(NH_4)_2SO_4$ solution with 28 wt% of NH_4NO_3 saturated at 50°C was prepared and 16.2 g of seed $(NH_4)_2SO_4$ crystal with mean size of 500μm was added at the moment the cooling started. The optimum cooling curve was determined as described in section 3 for $\eta_{max} = 0.5$. The solution temperature was controlled using BMPC (batch model predictive control)(Lee *et al.*, 1999) which is cascaded with a PID controller for jacket temperature control. BMPC is a special batch process control technique that can achieve highly precise tracking, as the batch run is repeated, despite model uncertainty and repeated disturbances. Until the precise temperature tracking is attained, batch runs were made with only water in the vessel. After precise tracking, crystallization was started. Thanks to BMPC, crystallization could be performed under

a highly reproducible temperature tracking condition with average tracking error of less than 0.04^oC with maximum deviation of about 0.3^oC.

The final crystal product was assorted with standard sieves and the weight for each size interval was measured.

6. RESULTS AND DISCUSSION

Figure 12 shows a resulting size distribution of the final crystal product. Although some small size crystals below $400\mu m$ were observed, the amount is not significant.

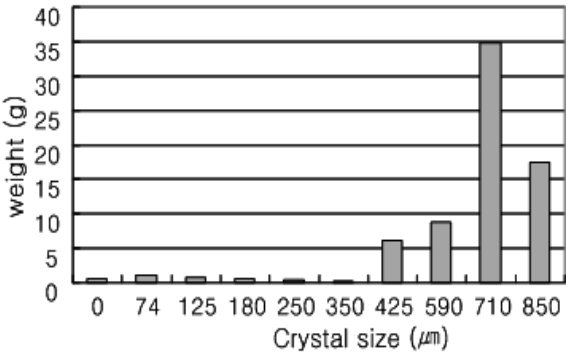

Fig. 12. Final crystal product size distribution: $L_{s_0} = 550\mu m$, $W_{S_0} = 8.1 g/kg$ solution.

A typical method to assess the uniformity of crystal size distribution is via the coefficient of variance defined by

$$CV = 100\left(\frac{L_{84\%} - L_{16\%}}{2L_{50\%}}\right) \qquad (10)$$

When CV is less than 20%, the crystal size is considered uniform enough in general. For our case, $CV = 16\%$ was obtained, which supports that primary homogeneous and also secondary crystallization was not significant during the operation. The weight average size of the crystal was 780μm and the total recovered crystal weight was 70.1 g. The predicted size and weight gain by the model equations (5) and (6) were 800μm and 78.7 g, respectively. Considering the weight loss of the crystal product due to adhesion on the vessel wall and filter paper and dissolution during washing, the experimental results are regarded to show quite good agreement with the theoretical prediction.

7. CONCLUSIONS

Through this study, a dynamic model for the metastable limit in cooling crystallization has been proposed and an optimum cooling curve has been calculated on the basis of the model. An interesting consequence is that the optimum cooling curve can have a sharp temperature decrease during an initial period without inducing homogenous crystallization, which is contrary to the usually practiced cooling curves. Experimental study supports, though not completely, the theoretical prediction and the validity of the proposed dynamic model for the metastable limit.

To draw a more concrete conclusion, it is necessary to carry out more experiments not only on the crystal growth but also on homogeneous nucleation. Those experiments are being under way.

REFERENCES

Choi, C. S and I. S. Kim (1990). Crystal growth of $(NH_4)_2SO_4$ in the ternary system $(NH_4)_2SO_4$-NH_4NO_3-H_2O. *Ind. Eng. Chem. Res.* **29**, 1558–1562.

Choi, C. S and I. S. Kim (1991). Controlled cooling crystallization of $(NH_4)_2SO_4$ in the ternary system $(NH_4)_2SO_4$-NH_4NO_3-H_2O. *Ind. Eng. Chem. Res.* **30**, 1588–1593.

Lee, K. S., J. Lee, I. Chin, and H. J. Lee (1999). A model predictive control technique for batch processes and its application to temperature tracking control of an experimental batch reactor. *AIChE J.* **45(10)**, 2175–2187.

Miller, S. M. and J. B. Rawlings (1994). Model identification and control strategies for batch cooling crystallizers. *AIChE J.* **40**, 1312.

Mullin, J. W., *Crystallization* 3rd ed., Butterworth Heine mann, Wiltshire.

Nývlt, J., R. Rychly, J. Gottfried, and J. Wurzelova. Metastable Zone Width of Some Aqueous Solutions. *J. Cryst. Growth* **6**, 151-162.

Nývlt, J., Induction period of nucleation and metastable zone width. *Collections of the Czechoslovak Chemical Communications* **48**, 1977-1983.